Characterisation of mechanosensory structures on the antennal flagellum in *Daphnis nerii*

Thesis submitted in partial fulfilment of the requirements of Five Year BS-MS Dual Degree Program at

Indian Institute of Science Education and Research, Pune

Gayathri K

20151052

IISER Pune

Under the supervision of

Dr. Sanjay. P. Sane

Insect Flight lab

NCBS, Bengaluru

CERTIFICATE

This is to certify that this dissertation entitled 'Characterisation of mechanosensory structures on the antennal flagellum in *Daphnis nerii*' towards the partial fulfilment of the BS-MS dual degree programme at the Indian Institute of Science Education and Research, Pune represents study/work carried out by Gayathri K at NCBS, Bengaluru under the supervision of Dr. Sanjay. P. Sane, Associate Professor, NCBS, Bengaluru during the academic year 2019-2020.

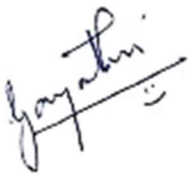

Dr. Sanjay. P. Sane
Associate Professor
NCBS, Bengaluru

Gayathri K

Date: 23 March 2020

DECLARATION

I hereby declare that the matter embodied in the report entitled 'Characterisation of mechanosensory structures on the antennal flagellum in *Daphnis nerii'* are the results of the work carried out by me at the Insect Flight lab, NCBS, Bengaluru, under the supervision of Dr. Sanjay. P. Sane and the same has not been submitted elsewhere for any other degree.

Dr. Sanjay. P. Sane
Associate Professor
NCBS, Bengaluru

Gayathri K

Date: 23 March 2020

ACKNOWLEDGMENTS

First and foremost, I would like to thank Dr. Sanjay Sane for giving me the opportunity to work in Insect flight lab. His constant guidance and support were immensely helpful through the course of my project. The lab environment he has created along with his students is truly commendable. His spirit and enthusiasm for science are very inspiring and I am glad to have had the opportunity to work with him.

I would like to thank Maitri for being there, from the first day, to patiently teach me every single detail pertaining to the work in the lab. The title ‘supreme leader of the lab’ suits her perfectly. I am grateful to Partha for taking time away from his work to guide me. The electrophysiology experiments would have been impossible without him. I would also like to thank the other lab members, Chinmayee, Agnish, Payel, Abin, Simran, Subha, Shipra, Vidur, Umesh and Girish for making me part of the clan. They were always ready to help and guide me at different stages of the project. I have learned a lot from each of them. The countless discussions with them over *chai* about science and life always gave me something to mull over. I wish to express my gratitude to Allan and Maruti for keeping our moths happy and fat. The lab and its people have been like my home away from home, my happy place during the time I have been part of it. Our collective sense of humour, though unbearable at times, has left me laughing at the end of most days and I am extremely grateful for that.

I am very grateful for the supportive network provided by other labs in NCBS. I am thankful to Upi lab and Ladher Lab, for allowing me to borrow necessary equipment and materials which were crucial for the completion of certain experiments. I am indebted to the Mechanical and Electronics workshop at NCBS for their help with the experimental setups and circuits. I am also grateful to my TAC member, Dr. Anand Krishnan for his valuable suggestions and feedback.

I thank my friends for the wonderful 4 years I spent at IISER Pune. You guys have stuck with me through thick and thin. I thank my professors, batchmates and classmates from biology courses for creating a conducive atmosphere for debate, discussions and learning.

Finally, I am eternally grateful to my parents, brother and grandparents for being there for everything. Their undying love and unwavering support keeps me going.

CONTENTS

LIST OF FIGURES AND TABLES

ABSTRACT

The insect antenna is a multi-sensory organ, which senses odour, mechanical as well as thermal and humidity cues. The significance of mechanosensory feedback provided by antennae has been particularly highlighted in recent studies. Mechanosensory cues such as touch, sound, airflow, aerial rotations etc. are detected by the exquisitely sensitive Johnston's organs situated in the basal antennal segments. Another set of mechanosensors, antennal hair plates or Böhm's bristles, have been implicated in precise positioning of the antennae through proprioception, especially during locomotion. The mechanosensory cues transduced by these sensors are crucial for flight stability. Although the role of Johnston's organs and Böhm's bristles has received much attention, there are also several mechanosensors along the length of the antennal flagellum in moths, whose role is relatively unexplored. We know very little about the nature and distribution of mechanosensors along the flagellum, or their role in insect behaviour. In this thesis, we explore the morphology and function of flagellar mechanosensors in the study system of the Oleander hawkmoth (*Daphnis nerii*), using various techniques such as scanning electron micrographs, neural dye fills, confocal microscopy, behavioural assays and electroantennography. Scanning electron micrographs revealed the location of putative mechanosensors on every annulus, except the first few annuli. Fluorescent dye labelling of sensory neurons innervating the flagellum (whole flagellar fill) revealed central projections in the ipsilateral Antennal Lobe (AL), ipsilateral Antennal Mechanosensory and Motor Centre (AMMC), ipsilateral and contralateral Sub-Esophageal Zone (SEZ), and also into the mesothoracic ganglia. We hypothesized that flagellar mechanosensors mediate specific behaviors such as antennal grooming by insects, but our attempts to assay these behaviours were unsuccessful. We also tried to measure their response to mechanical stimuli such as wind, using electroantennography (EAG). Together, these data describe the nature and distribution of flagellar mechanosensors in *Daphnis nerii*.

1. INTRODUCTION

Insect antennae sense and respond to diverse cues in their environment including odours, temperature, moisture and air speed (Schneider, 1964). Although antennae serve as the primary olfactory organ of the insect, the mechanosensory feedback they provide to the animal is both crucial and diverse across species. Antennal mechanosensors in cockroaches, crickets and stick insects mediate escape responses and object-guided orientation (Burdohan and Comer, 1996; Okada and Toh, 2000; Schütz and Dürr, 2011; Staudacher et al. 2005). In social insects, antennal mechanosensory structures mediate tactile communication (Tautz and Rohrseitz, 1999; Ettorre et al., 2004) whereas in flying insects such as locusts, moths and bees, they are crucial for flight stability (Arbas, 1986; Sane et al., 2007; Khurana and Sane, 2016). Hawkmoths and honeybees possess whip-shaped “flagellar” antennae, consisting of three parts: the basal scape, medial pedicel and the distal flagellum (Schneider, 1964). Studies on the tobacco hornworm *Manduca sexta* have demonstrated that the mechanosensory structures (Böhm’s bristles on antennal scape and pedicel and Johnston’s organs in pedicel-flagellar joint) are essential for stable flight (Sane et al., 2007). These studies have also elucidated the role of Böhm’s bristles in antennal positioning during flight or walking. Johnston’s organs sense diverse mechanosensory cues ranging from low frequency signals from airflow or gravity (Kamikouchi et al., 2009; Yorozu et al., 2009), to high-frequency signals due to antennal vibrations (Dieudonné et al., 2014) during aerial turns (Sane et al., 2007) or sound (Kamikouchi et al., 2009; Yorozu et al., 2009). Unlike the basal antennal mechanosensory structures, however, the nature and distribution of flagellar mechanosensory receptors have received less attention in Lepidoptera. Their presence along the flagellum may help mediate tactile sensing to detect surfaces, presence of foreign particles that interfere with olfaction, mites, etc. The flagellum is especially a site of interest as it covers the largest surface area on the antenna, with continual exposure to the external environment.

From a functional perspective, flagellar ablation causes loss of flight stability, but mechanical reattachment restores flight control in moths, even though the flagellar nerve remains in a severed state. This suggests that flagellar mechanosensory feedback is not essential for stable flight, unlike the feedback from Johnston’s organs (Sane et al., 2007;

Dieudonné et al, 2014). However, flagellar mechanosensors may be involved in detecting the presence of minuscule undesirable particles on the antennae that interferes with sensory acuity. In a variety of insects, grooming behaviour is induced by presence of undesirable substances like chalk dust on the antennae (Hlavac, 1975). Previous studies have demonstrated the relevance of antennal grooming in enhancing its olfactory acuity (Böröczky et al., 2013), preventing ectoparasites (Zhukovskaya et al., 2014) and spreading cuticular antimicrobial secretions on the body (Lusebrink et al., 2008). Antennal grooming has also been reported in moths (Callahan and Carlyle, 1971; Barry and Nielsen, 1984), and likely helps remove impurities on the antenna that could interfere with olfaction. It would be interesting to study the role of flagellar mechanosensors in eliciting antennal grooming.

In my project, I describe the morphology, neuroanatomy and behavioural role of flagellar mechanosensory structures in the Oleander hawkmoth (*Daphnis nerii*) study system. At the initial stages, we surveyed the morphology of the flagellar mechanosensors in hawk moths using Scanning Electron Microscopy (SEM), by characterizing their distribution and density along the flagellum in both female and male moths, to explore the sexual dimorphism in the antennal flagellum. Additionally, we mapped their central projection patterns through fluorescent dye labelling of the underlying neurons by staining whole antennal nerve innervating the flagellum. To study the role of flagellar mechanosensors in triggering antennal grooming behaviour, we tried to develop a behavioural assay. Environmental cues are transduced into electrical impulses or action potentials by different types of sensors. By studying the electrophysiology of a sensor during stimulus exposure, we can gain insights into its encoding properties. We tried to characterize the neural response to mechanical stimuli by sensory neurons innervating antennal flagellum and as the first step, conducted EAG (electroantennography) recordings on the hawkmoth antennae. The EAG response recorded on the excised antenna shows an overall voltage response that is a summation of the responses of all mechanosensory sensillae.

2. MATERIALS AND METHODS

2.1 Moth Culture

Daphnis nerii occur naturally in Peninsular India. Larvae of the Oleander hawk moth, *D. nerii*, were reared in our laboratory at the National Centre for Biological Sciences, Bangalore, India. The larvae were reared on fresh leaves of *Nerium oleander*. Once the larvae entered the pupal phase, we transferred them into mesh boxes with sawdust flooring. The emergent adult insects were maintained on a natural day-night cycle. The life cycle from egg to a mature adult takes about 40-45 days in *Daphnis nerii*. From every batch, we kept aside a few males and females in an equal sex ratio to serve as breeding pairs and provided them with host plants. We collected the eggs laid by the mated females on the leaves of these plants and transferred them into plastic boxes with fresh leaves of *Nerium oleander*. We regularly introduced wild-caught *D. nerii* at a larval stage into the culture to prevent inbreeding depression.

2.2 Scanning Electron Microscopy (SEM)

For SEM imaging, we chose adult moths of age 0-2 days after emergence. Antennae (female and male antennae) were excised at the scape and fixed in 4% PFA for 12-14 hours at room temperature of 25ºC. The tissue was taken through dehydration in ascending grades of alcohol (10%, 20%, 30%, 40%, 50%, 60%, 70%, 80%, 90%, and twice in 100%) for 10 min each, followed by dehydration of the sample through Critical Point Drying (CPD ; Leica EM CPD 300 Critical Point Dryer, Leica microsystems, Wetzlar, Germany) to prevent shriveling. This was followed by coating with Gold/Palladium alloy of 10nm thickness using a sputter coater. This protocol required multiple rounds of standardizations in terms of orientation, length and thickness of Gold/Palladium alloy during sputter coating. After trying out leading edge, trailing edge and sideways (boundary of leading and trailing edge exposed) orientations, we opted for sideways orientation as this provided a clear view of the base of sensors. The antennae were cut into approximately 3 pieces since the curvature of the flagellum hindered sample mounting. The sample pieces were mounted onto the carbon tape on an aluminium stub. Sample was imaged in FESEM using SE2 detector (Zeiss Merlin Compact VP/Zeiss Gemini SEM,

Germany). The images were used to count the number of putative mechanosensors on each flagellar annulus. A putative mechanosensor was considered only if the sensilla base was clearly visible having a characteristic circular membrane at the base described in Schneider, 1964.

2.3 Fluorescent dye labelling of sensory neurons

0-1 day old Adult hawk-moths (of both sexes) were cold anesthetized and placed inside a plastic tube, immobilized using dental wax. We allowed the head of the moth to move and manually extended the proboscis to enable feeding. For the fluorescent labelling, we used two water soluble dextran dyes; Texas Red (3000 MW; lysine fixable; emission at 615 nm; excitation at 595 nm, Thermo Fisher Scientific) and Alexa fluor 488 (10,000 MW; Anionic; emission at 519 nm; excitation at 495 nm; Thermo Fisher Scientific).

We could not ablate and fill individual flagellar mechanosensors because the putative mechanosensors we found are present on the flagellum amidst chemosensors making it look indistinguishable under the light microscope thereby increasing the likelihood of ablating and filling a chemosensor. Therefore, we dye-filled the whole antennal nerve innervating the flagellum. To achieve this, we followed the fluorescent labeling protocol for mechanosensors at the base of the antennae that have been standardized in previous studies (Krishnan et al, 2012; Sant and Sane, 2018). We first standardized the dye-loading procedure. The antennae were affixed to the head using dental wax to restrict flagellar movements during the protocol. For dye-loading, the cuticle of the flagellum at ~5-6th annuli from the pedicel was scraped off with a micro-knife to make a window exposing the antennal nerve. This method ensured minimal haemolymph discharge during the procedure. The nerve was then severed using the micro-knife and a drop of distilled water added to the region to cause swelling of the axons, thereby enhancing dye uptake (Altman and Tyrer, 1980). After water absorption, a few drops of concentrated dye solution of Texas Red were added to the region 3-4 times at regular intervals.

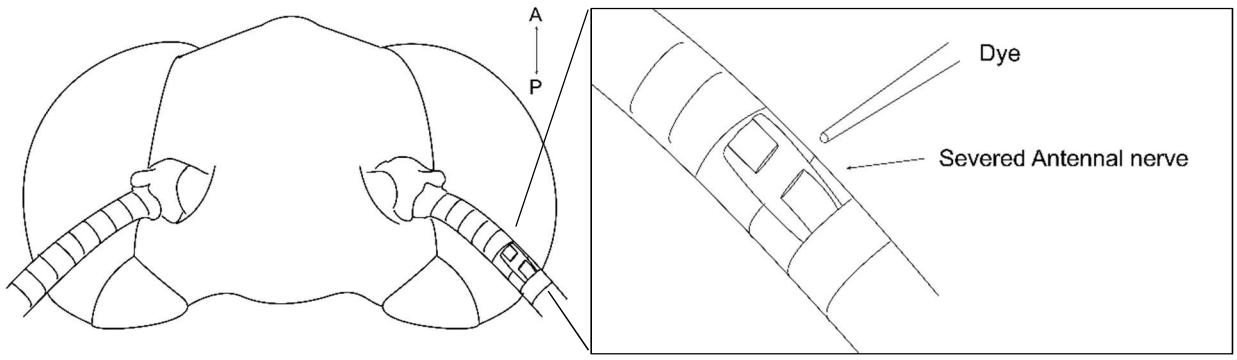

Fig 1: Dye-filling protocol: *For dye filling, a window exposing the antennal nerve was made and dye was filled into the cavity after the nerve was severed. A = Anterior, P = Posterior*

Across diverse insects, the mechanosensory neurons underlying Johnston's organs and Böhm's bristles project into a region of the brain called the AMMC (**A**ntennal **M**echanosensory and **M**otor **C**enter) (Homberg et al., 1989; Krishnan et al.,2012; Sant and Sane, 2018; Sant and Sane 2019). In moths, the neuropil of the AMMC is fused with surrounding areas of the protocerebrum and sub esophageal ganglion and its boundaries are ill-defined. The arbors of mechanosensory Böhm's Bristles and Johnston's organs hence offer the best frames of reference relative to which we can locate the arbors of the flagellar mechanosensors. Hence, we followed the strategy of simultaneously labelling Böhm's Bristles (or Johnston's organ) and flagellar nerves with different fluorescent dyes to provide a reference for the projection region. Alexa Fluor 488 was used for Johnston's organs / Böhm's bristles, whereas Texas Red was used for labelling flagellar nerves. To label the Böhm's bristle neurons, one of the scapal fields was ablated using a microknife and coated with Alexa Fluor 488 dissolved in distilled water. To trace the scolopidial sensillae of the Johnston's organs, a small region of the pedicellar-flagellar joint was exposed and a minutien pin was used to injure the underlying scolopidial units. After this, the region was filled with Alexa Fluor 488 dissolved in distilled water. In both cases, a drop of distilled water is placed on the injury site before dye addition. There were two groups of dye-filling done for the comparison. First group of moths had fluorescent dye labelling of Böhm's Bristles and flagellar neurons (BB + FN) and the second group had Johnston's organs and flagellar neurons (JO + FN).

The insects were kept alive in an aerated and humid container for 24-30 hours for sufficient diffusion and labelling of the dye. When the preparation consisted of thoracic ganglia, this period was extended to 48 hours. After 24 hours, the sample was fixed in 4% PFA (Paraformaldehyde) for 12-14 hours at room temperature of 25°C. Brain and thoracic ganglia were dissected out in insect saline and dehydrated for 10 min in each of alcohol series (50%, 60%, 75%, 90%, 100% ethanol twice). Tissue sample was cleared in Methyl Salicylate for 10-15 min. The moth brain was imaged using 10x and 20x objectives using a laser-scanning confocal microscope (Olympus FV1000, Central Imaging and Flow Cytometry Facility (CIFF), NCBS, Bangalore, India).

2.4 Behavioural Assay pilot experiments

Antennal grooming is elicited by the presence of pollen on the antennae in *Heliothis zea* (Callahan and Carlysle, 1971). We followed a similar protocol to induce grooming in the adult *D.nerii*. One-day/two-day old moths were placed inside a wire mesh cage (~30cm x 30cm x 30cm). The insect was cold-anesthetized and its flagellum painted/sprinkled with a variety of materials to induce grooming response i.e. mustard pollen, polysynthetic resin adhesive (Fevicol MR, Pidilite Industries Limited) and chalk dust. The anesthetized insect was placed in the cage. A camera recorded its movements from its placement until it took its first flight post-anesthesia. Each moth underwent only one trial. These recordings were done at dusk (17:30 to 19:30 hrs) under IR light. Chalk dust was used in the first set of experiments since it was readily available. Unfortunately, despite several trials, this stimulus failed to evoke any grooming response in the moths, perhaps because most of the coated pollen dust fell off the flagellum. However, even after we changed the stimulus to stickier particles, none of the animals showed antennal grooming despite repeated trials (n=6). This line of experimentation was therefore abandoned, and we decided to instead directly record from the antennae, as described below.

2.5 Electroantennography (EAG)

Electroantennography (EAG) is a widely used technique in entomology to study how the insect antennae senses odours. This helps in the determination of the receptive range of an insect's antenna. In EAG, electrical potential difference between tip and proximal

sections of the antennal flagellum is measured. The EAG response amplitude represents the sum of dendritic potentials elicited by a stimulus and is correlated to the overall number of sensory neurons that are sensitive to that stimulus (Schneider, 1957; Kaissling and Thorson, 1980; Kaissling, 1995).

Electrodes: We used silver wire (127 µm; A-M Systems, Inc., Sequim, WA, USA) as electrodes. Before the recording, the electrode tip was chloridised by immersion in 4% bleach (Sodium Hypochlorite) for 15-20 min until it turned gray. This produces a silver–silver chloride (Ag/AgCl) electrode that is non-polarisable. Non-polarisable electrodes are reliable for electrophysiological recordings because current passes freely across electrode/electrolyte junction and do not develop overpotentials resulting from the flow of current through the electrode. This was followed by rinsing off the bleach from the tips using distilled water.

Stimulus: Mechanosensory stimuli were given in the form of air puffs. The air puffs were regulated through two-way solenoid valves which let air go in the 'ON' position and disallowed the passage of air in the 'OFF' position (Fig 2). We also recorded responses to odour stimuli for comparison with the response to mechanosensory stimuli since absolute values of parameters associated with the response could vary across different sample preparations. We used nitrogen as a carrier gas to ensure that the odour molecules are not oxidized. The volatile compound Linalool was chosen as the odour to be used since it is a naturally occurring terpene alcohol present in floral scent and evoked strong EAG response during pilot experiments. Nitrogen goes into the flowmeter where the air flow rate is maintained at ~0.2 L/min. The air (blank or laden with odour) reaches the antennae after passing through the 2-way solenoid valves which is driven by a custom-made circuit in Fig 3. We used a small piece of filter paper loaded with <1 mL of Linalool as odour source. The odour laden paper was placed in an HPLC vial of 1.5 mL (USP type). A blank vial was used to serve as control in the other line. Two (22 X $1_{1/2}$ - gauge needle) hypodermic syringe needles used to serve as inlet and outlet. This setup has been described schematically in Fig 2. All trials were conducted at room temperature (~25 ℃). The nozzle through which air puffs reach the flagellum was kept at a distance ~ 1.5 cm.

Sample preparation: Antenna was surgically removed from a male moth which was 0-1 day old. The cut was made at 3rd-4th annulus from the pedicel and tip of the flagellum. In this way, we eliminated the responses coming from the basal mechanosensors (Böhm's bristles and Johnston's organs). The incisions made at the ends of the antennae were done such that the electrodes were in contact with the internal haemolymph. This was immediately followed by inserting the chlorinated electrode tips of the two-pronged Ag/AgCl electrode-recording probe. The antenna was set up such that the boundary of the leading and trailing edge (Fig 4) faces upwards. This was done to maximize the exposure to odour puff by the chemosensors and the air puff by the putative mechanosensor. The orientation of the flagellum was adjusted under a light microscope. This preparation was stuck to a platform using double tape to minimize movement of the flagellum during the stimulus delivery.

Experimental setup: The platform with the flagellum was kept on the anti-vibration table. Stimulus duration and inter-trial interval (ITI) to be run were controlled using a custom-written code operated in MATLAB (MATLAB *ver R2019a*, The MathWorks Inc., Natick, Massachusetts) During electrophysiological experiments, the signal going into the 2-way solenoid valves were independently digitized.

Data Acquisition and Analysis: The signal was filtered using a pre-amplifier (Astro-Med Inc., Grass, P55 A.C. Pre-amplifier; band-pass filtered 0.3Hz to 300 Hz; gain= 2×) kept close to the electrodes. The signal then went into an amplifier (10,000×). The EAG responses were sampled at 3 kHz via a data-acquisition card (USB-6229, National Instruments, Austin, TX, USA) and stored for offline analysis. The AC noise of 50 Hz superimposed on the signal was removed digitally. The data was compiled and plotted on MATLAB. The following quantities were calculated from the data using a custom-written MATLAB code.

i. Time of onset of response
ii. Peak-to-peak amplitude
iii. Area under the curve
iv. Response time
v. Slope of the drop in voltage

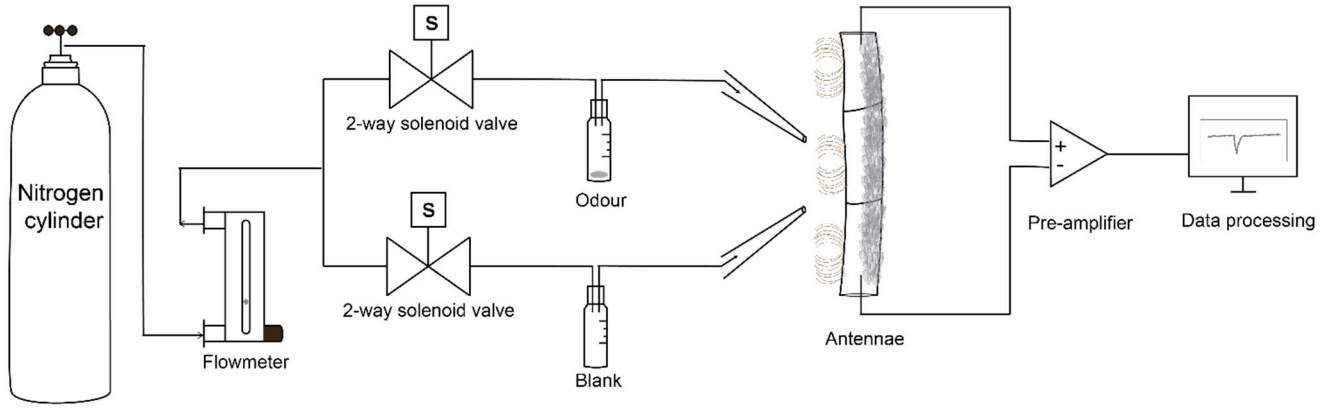

Fig 2: EAG stimulus delivery system: *Nitrogen goes from the cylinder into the flowmeter where the air flow rate is regulated at 0.2 L/min. Air (Nitrogen) is split into two distinct lines (odour and blank) . Each line goes into a 2-way solenoid valve which can be switched ON/OFF to allow/disallow the passage air respectively. The final air outlet is kept ~1.5 cm away from the antenna.*

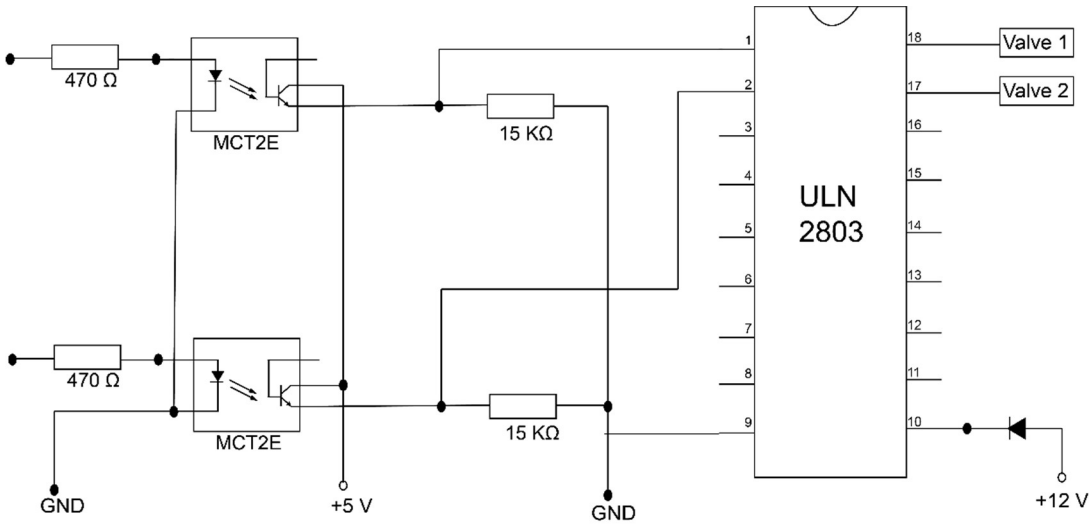

Fig 3: Circuit diagram of the driver system for the 2-way solenoid valves (denoted by valve 1 and valve 2): *Only one valve (either Valve 1 or Valve 2) is open at a time. When a valve is ON, it is open and air goes into its respective vial (blank/odour). Valves are operated to provide air puff controlled by custom written code in MATLAB. MCT2E is a phototransistor optocoupler. The ULN2803A device is a 50 V, 500 mA Darlington transistor array. GND denotes grounding.*

3. RESULTS

3.1 Scanning Electron Microscopy (SEM)

The antennal flagellum of *D. nerii* has two sides; the side that faces forward during the moth's forward flight is called the 'leading edge' and opposite side which is fully covered with flat scales called the 'trailing edge' (Fig 4, left).

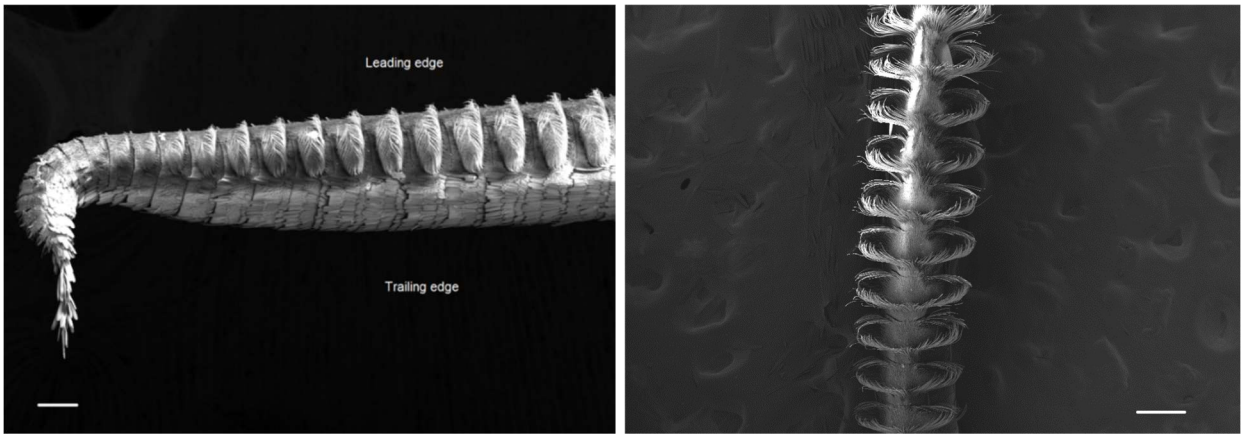

Fig 4: Antennal flagellum in *D.nerii*: (Left) Two opposite edges of the male antennal flagellum. *Leading edge contains the chemosensors and the trailing edge is mostly covered by scales.*
(Right) Leading edge of the male antennal flagellum. *Note the array of chemosensors. This is absent in female antennal flagellum, making this a sexually dimorphic trait. Scale bar = 200 µm*

In male antennal flagellum, we observed a distinct arrangement of chemosensors on the leading edge of every annulus (Fig 4, left). On every annulus, there are two U-shaped patterns made by the chemosensors on the leading edge near the boundary between the leading and lagging edge of the antennae (Fig 4, right). The U-shaped patterns on either side of the leading edge are connected by the chemosensors towards the proximal side (towards the head) of the annulus. This arrangement is similar to that described in the antennal flagellum of *Manduca sexta* (Tobacco hornworm moth) in which this class of chemosensors have been identified as sensilla trichodea (s.trichodea). We do not observe this distinct array of chemosensors on the female flagellum of *D.nerii* (Fig 5).

Interestingly, in male flagella, we see the presence of a distinct sensor near the end of every U-shaped arrangement (Fig 6, left). Thus, there are two such sensors on every annulus (Fig 5). The putative mechanosensor is a spine-like external process with a characteristic cuticular wall of thickness ~1 μm surrounding it (Fig 6). The base structure (cuticular wall), shaft morphology (absence of any longitudinal or transverse ridges) and base width (~5-8 μm) of this sensor resembles that of sensilla chaetica type-I (Lee and Strausfeld, 1990). The length of the putative mechanosensor ranges between 30-70 μm.

Identification of this sensor comes with many constraints. This sensor is visible only in the orientation where the boundary of leading and trailing edge is facing upwards. In addition to this, its location amidst the long chemosensors (s.trichodea) poses a challenge as it occludes the view of base of the sensor, which is critical for identification of the putative mechanosensor. This sensor is distinct from the neighbouring sensilla trichodea in terms of average shaft length, shaft morphology, base morphology and base width. This feature is present consistently across all annuli excluding the first few proximal annuli. Each of these sensors has a characteristic raised cuticular wall of thickness ~1 μm surrounding it (Fig 6). The base structure (cuticular wall), shaft morphology (absence of any longitudinal or transverse ridges) and base width (~5-8 μm) of this sensor resembles that of sensilla chaetica type-I (Lee and Strausfeld, 1990). The length of the putative mechanosensor ranges between 30-70 μm.

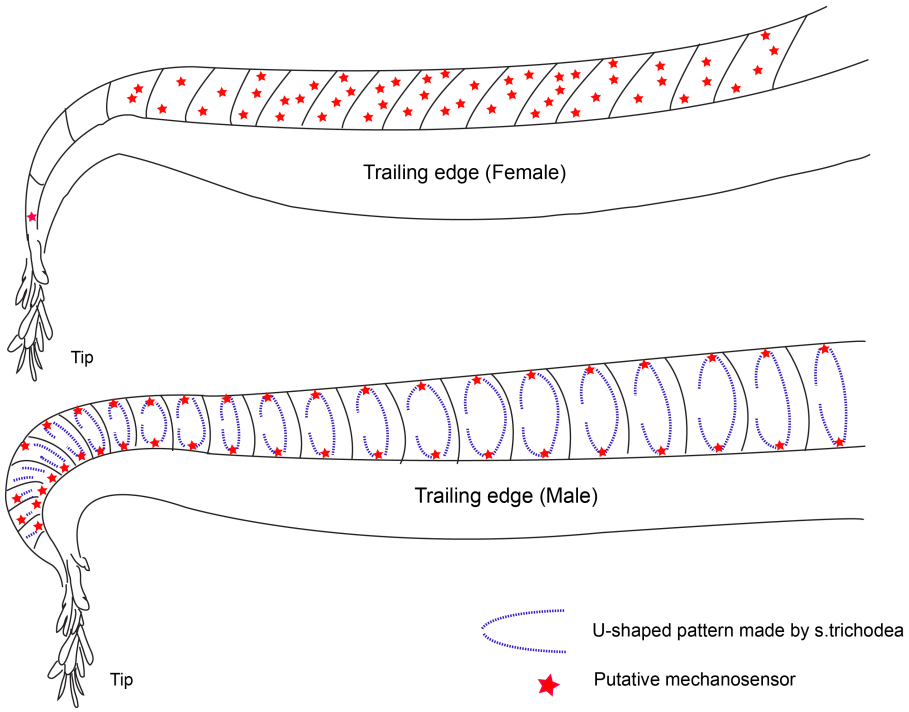

Fig 5: Schematic representation of location of the putative mechanosensors (red stars) on the male and female antennal flagellum. *In male flagellum, the putative mechanosensors are found amidst the chemosensors (s.trichodea) near the periphery of leading edge denoted by blue markings here. In female flagellum, it is found towards the center of the leading edge.*

In female flagellum, these putative mechanosensors are present towards the center of the leading edge of the antennae (Fig 6, right) as compared to the male flagellum. Their numbers range between 1 and 4 per annulus across the antenna.

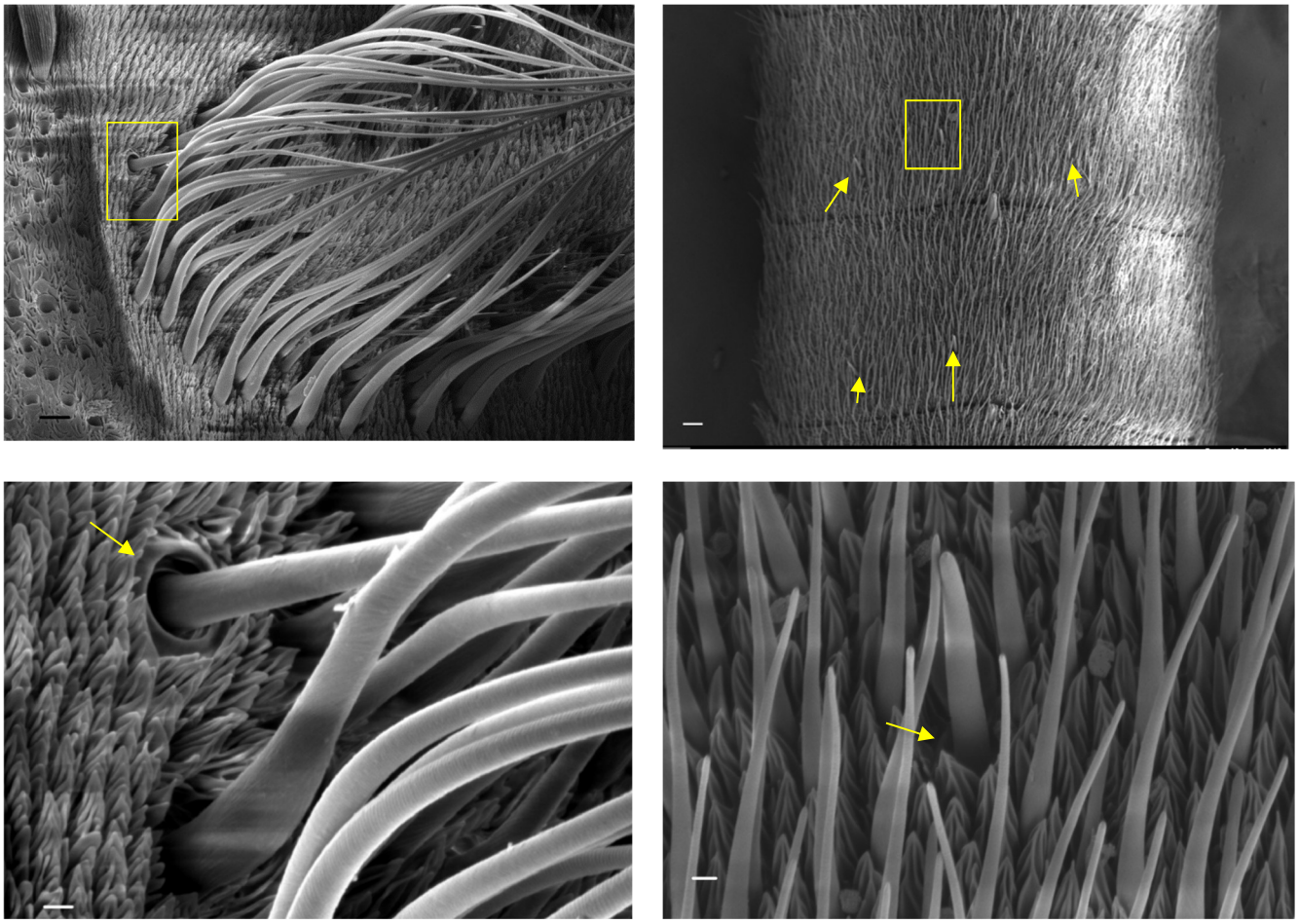

Fig 6: (Left) Male antennal flagellum: *(Above) boundary of leading and trailing edge of an annulus. Scale bar = 10 µm. (Below) enlarged view of the putative mechanosensor Scale bar = 2 µm. Note the cuticular wall around base of the sensor.*

(Right) Female antennal flagellum: *(Above) Leading edge of female antennal flagellum containing putative mechanosensors (yellow arrows). Scale bar = 20 µm. (Below) enlarged view of the putative mechanosensor. Scale bar = 2 µm*

In addition to the leading edge, the tips of both male and female antennae seem to house the putative mechanosensors (Fig 7).

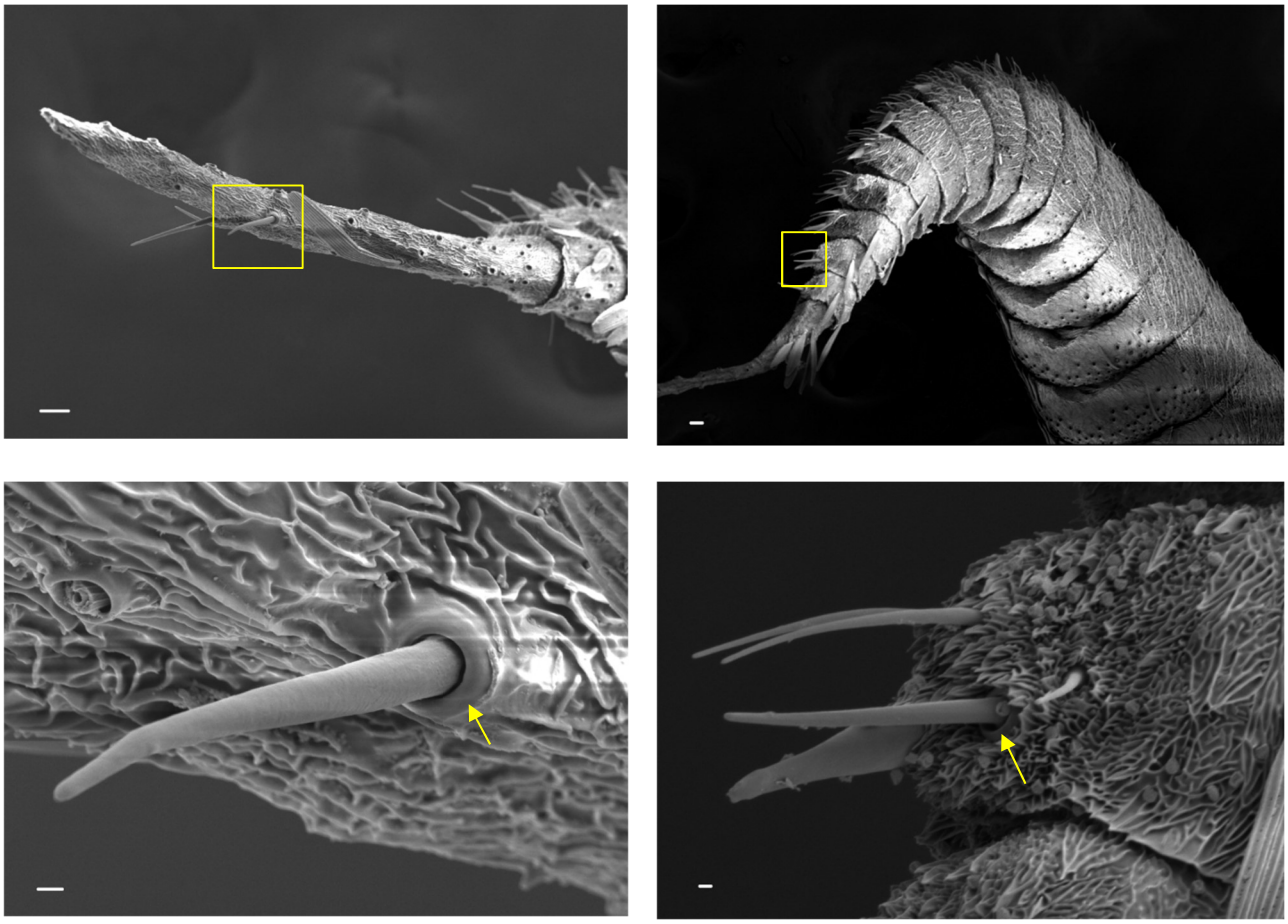

Fig 7: (Left) Tip of the Male antennal flagellum: *(Above) Sensors on the tip of the Male antennal flagellum. Scale bar = 20 µm. (Below) enlarged view of the putative mechanosensor at the tip. Scale bar = 2 µm*
(Right) Tip of the female antennal flagellum: *(Above) Tip of the female antennal flagellum. Scale bar = 20 µm. (Below) enlarged view of the putative mechanosensor at the tip. Scale bar = 2 µm.*
Yellow arrow: cuticular wall around the base of the sensor.

3.2 Neuroanatomy

Central Nervous System of Daphnis nerii

The insect brain is positioned above the esophagus, in the dorso-posterior part of the head capsule. The CNS of *D. nerii* is composed of the brain and ventral nerve cord (VNC). The nomenclature employed for identifying and labeling parts of CNS has been adopted from *Eaton, 1974* and *Ito et al, 2014* (Fig 9).

The brain can be divided into the following neuromeres; protocerebrum (PR), deutocerebrum (DE), tritocerebrum (TR) and the Sub-esophageal zone (SEZ) (Fig 8). The optic lobes (OL) on the lateral parts of the moth brain form parts of the protocerebrum. The deutocerebrum contains the antennal lobe (AL) along with the antennal nerve (AN) located ventrally and the antennal mechanosensory and motor center (AMMC). Tritocerebrum lies below the deutocerebrum. The sub-esophageal zone (SEZ) lies below tritocerebrum and spans from either side of the oesophageal foramen (OF) till the beginning of cervical connective. In moths, these neuromeres are fused together with unclear boundaries. The ventral nerve cord which is situated under the esophagus, consists of the cervical connective, prothoracic ganglia (T1), mesothoracic ganglion (T2) and metathoracic ganglion (T3) as we go towards the posterior end of the CNS. The cervical connective joins the brain and the prothoracic ganglia (T1). The mesothoracic ganglion (T2) is fused with metathoracic ganglion (T3) while the prothoracic ganglion (T1) is linked to this complex by a paired connective.

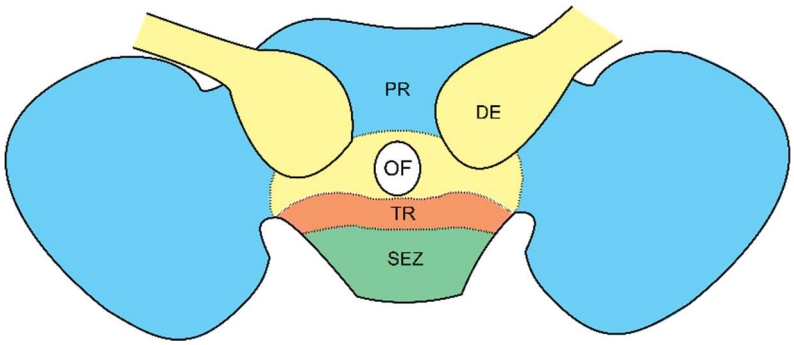

Fig 8: The moth brain is separated into various neuromeres: (PR) Protocerebrum, (DE) Deutocerebrum, TR (Tritocerebrum) and SEZ (Sub-esophageal Zone). *Due to fusion of these neuromeres, the boundaries are difficult to define. This figure is based on Ito et al., 2014.*

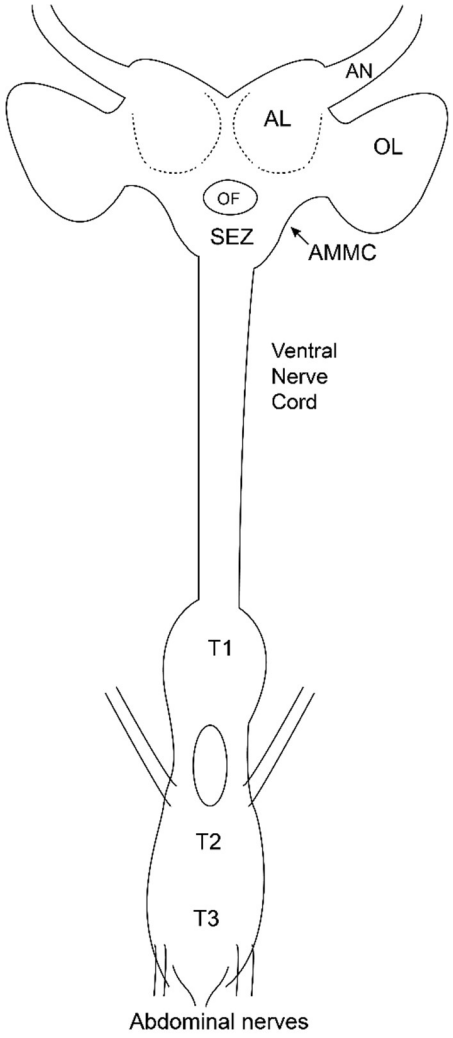

Fig 9: Central nervous system of *Daphnis nerii*.

Abbreviations

AN: Antennal Nerve

AL: Antennal Lobe

OF: Oesophageal Foramen

OL: Optic Lobe

AMMC: Antennal Mechanosensory and Motor Center

SEZ: Sub-Esophageal Zone

T1: Prothoracic ganglion

T2: Mesothoracic ganglion

T3: Metathoracic ganglion

Fluorescent labeling of antennal sensory neurons

Antennal nerve innervating the flagellum has arbors in different areas of the brain (Fig 10), including a group of neurons that innervates the ipsilateral antennal lobe of the brain, and another which bypasses the antennal lobe, and arborizes in the ipsilateral AMMC (Fig 10). We also observed a projection to the ipsilateral SEZ (Sub-Esophageal Zone) (Fig 10) with a contralateral branch that appears to cross the midline.

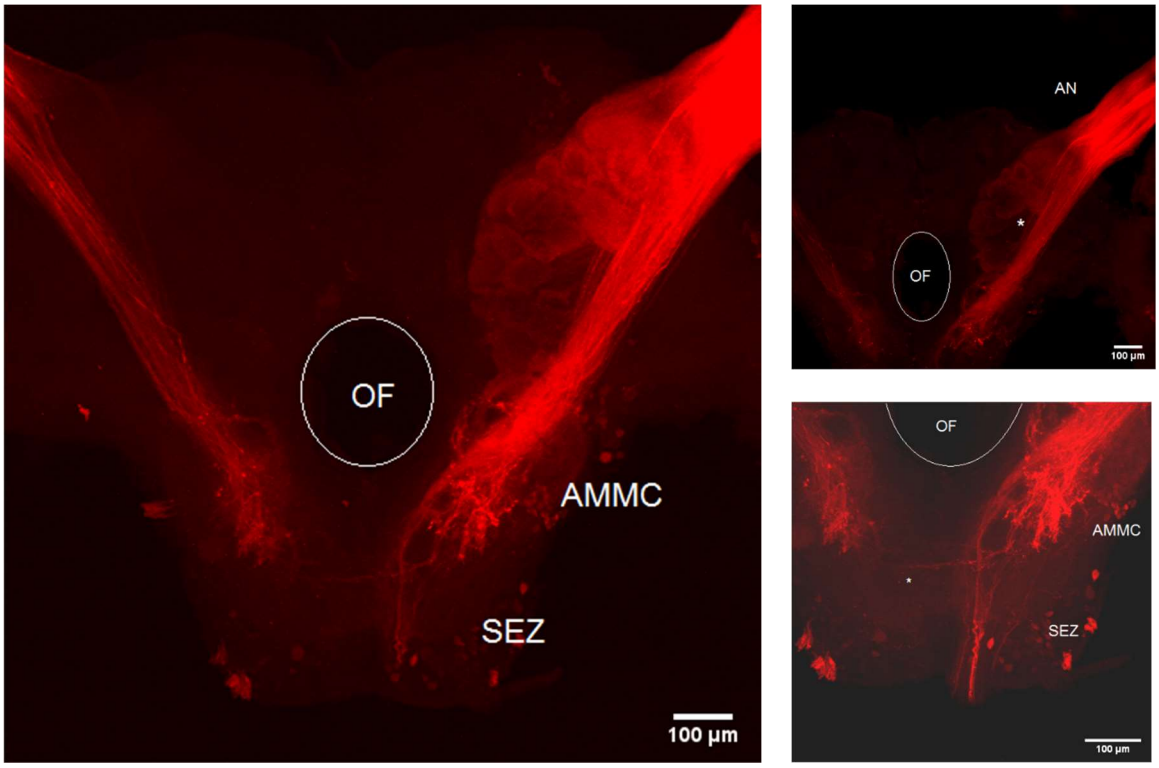

Fig 10: Neural projections of flagellar neurons in the hawkmoth brain: *(Clockwise from right) (1) Flagellar neurons have projections in the AL and AMMC. (2) Antennal lobe (*) is a site of extensive projection. (3) Closer look at SEZ shows contralateral projections (*) and axons going towards the cervical connective. Scale bar = 100 µm*

Two distinct axonal projections enters the ipsilateral cervical connective (Fig 11), and could be traced as far as the prothoracic ganglion (T1). From here, a neuronal tract extends towards the mesothoracic (T2) ganglion through the connective between T1 and T2. Unfortunately, the arbors or projections in the thoracic ganglia were somewhat unclear because of neuronal death, as indicated by blebbing in the sample, which occurs when the cell bodies are impacted and the insect is kept alive to wait for the dye to diffuse.

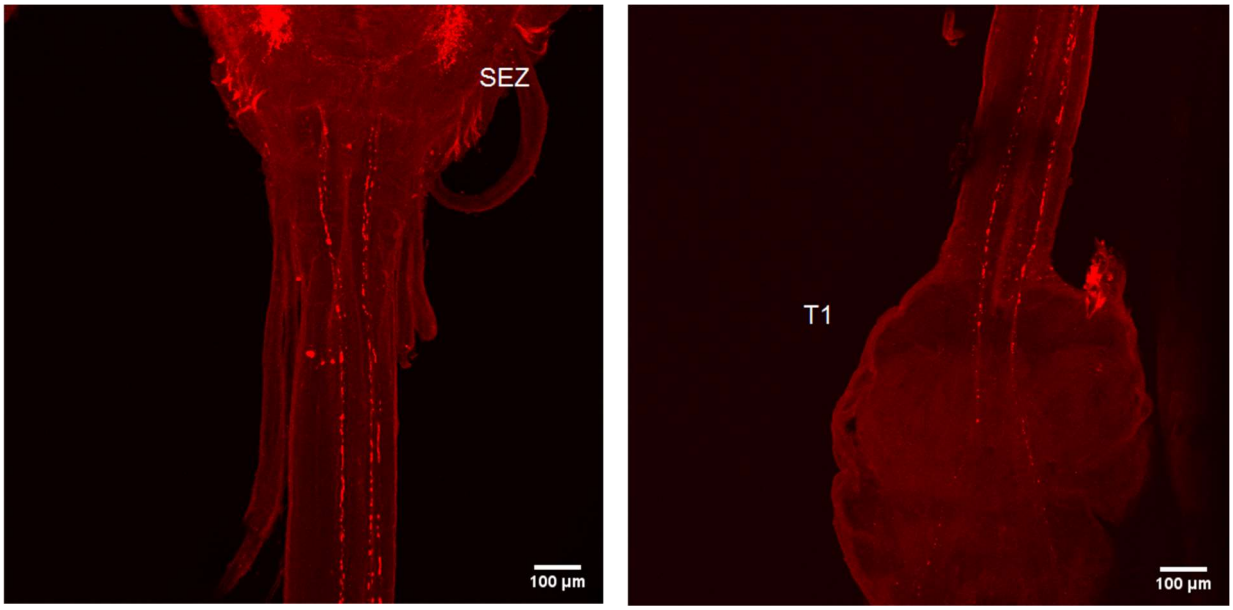

Fig 11: Axons from flagellar neurons in the ventral nerve cord *(Left) entering cervical connective (Right) entering prothoracic ganglion (T1). Scale bar = 100 µm*

The samples with double fills (BB+FN and JO+FN) shows neural projections of Böhm's bristles and Johnston's Organs. The neurons underlying the Böhm's bristles (Fig 12, left) and Johnston's organs (Fig 12, right) have their projections in the AMMC. These are in agreement with the previously demonstrated arbors of these mechanosensors (Sant and Sane, 2018). On comparison between Fig 12 and Fig 15, at a preliminary level, we can see that there are similarities in the region of projection in the brain between arbors flagellar nerve and BB/JO.

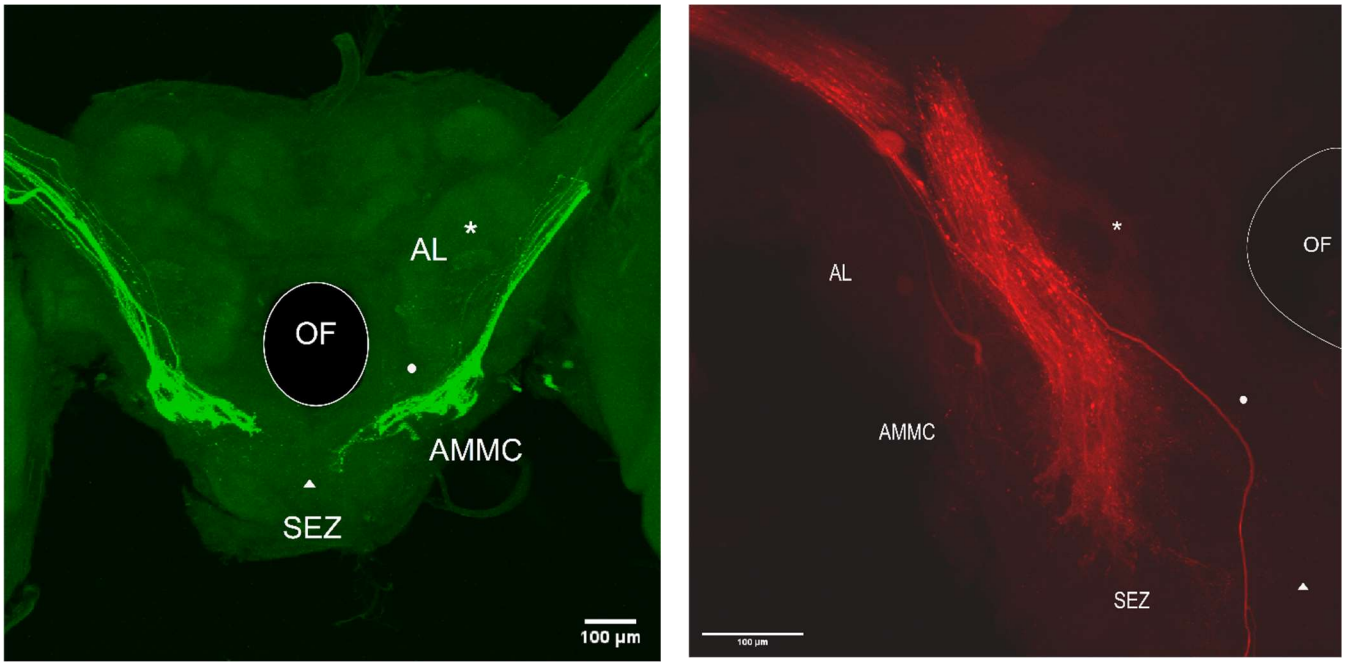

Fig 12: Neural projections of Böhm's bristles and Johnston's organs in hawkmoth brain. *(Left) Sensory neurons underlying the Böhm's bristles have arborisations in AMMC (solid circle). * = antennal lobe; solid triangle = SEZ region. (Right) Scolopidial cells from Johnston's organs have projections in the AMMC (solid circle) and go towards SEZ (solid triangle). Scale bar = 100 µm*

3.3 Electroantennogram (EAG)

The preliminary EAG studies showed that the male antennae responded to both odour and blank air puff. We could not see any significant differences between responses to odour puff and blank air puff (Fig 14, 15). When blank air puffs were given to the antennae, we saw responses which typically had two troughs (Fig 13). The odour puff on the other hand, evoked a consistent (Fig 14) drop in voltage after the onset of stimulus. These differences could be due to artifact in the response introduced due to the valve. Since the same valve was used across all blank air puff trials, artifact produced to the valve-specific dynamics would be reflected in all the responses. Although we recorded from a total of 5 antennae (from 3 moths), the quantitative comparative analysis used the data of only 1 antenna, because the comparative analysis (Fig 13) required that the sample be exposed to both odour puff and blank air puff. We calculated the parameters described in section

2.5 for one antennae over 10 trials each for odour puff and blank air puff stimulus, as described in the table below.

Parameter \ Stimulus	Odour Puff (Nitrogen + Linalool)	Blank Air Puff (Nitrogen)
	Mean ± S.E	**Mean ± S.E**
Peak-to-peak amplitude (μV)	76.16 ± 3.24	105.89 ± 1.85
Response Onset Time (ms)	47.13 ± 0.80	58.30 ± 4.37
Area under the curve (V.ms)	38.67 ± 1.53	56.32 ± 1.39
Response duration (ms)	218.03 ± 4.68	160.3 ± 2.24
Slope of the response curve (μV/s)	-6.92 ± 0.51	-2.90 ± 0.15

Fig 13: Parameters (Mean ± SE) derived from the EAG responses to odour puff and blank air puff. *These results were derived from the EAG response of 1 antenna elicited by odour puff (10 trials) and blank air puff (10 trials).*

One of the drawbacks of this experiment was that the air flow was not calibrated near the outlet where air puffs reaches the antennae. In future experiments, this calibration can be done using anemometer. This would be important for multiple reasons. First, we can determine the air flow rate at the point of release. Second, this would aid in detection of any errors in the dynamics of the solenoid valves. Third, it would help regulate the stimulus signal to ensure stable air flow throughout the pulse duration.

From the parameter calculations, we see that the EAG amplitude was higher in case of response to blank air puff (BLR) compared to that to odour puff (ODR). This is contradictory to numerous previous studies (Schweitzer et al., 1976; Park et al., 2002). Comparisons of the response onset time showed that the ODR was elicited faster than the BLR. This could been the result of large number of chemosensors exposed to the odour. However, we need a larger data set to ensure this pattern is present consistently across preparations. Area under curve signifies the sharpness and spread of the curve. The BLR had more area under curve compared to ODR. This could have been partially because of the higher amplitude of the BLR since area is affected by both the amplitude

and spread of the curve. BLR also typically exhibits two troughs which could also be contributing to the increased area. Response time is the period of time between the onset of response till it comes back to baseline activity. On an average, response time for BLR was smaller compared to ODR i.e. in case of BLR the sample took shorter time to come back to baseline activity. Slope of the response curve signifies the rate at which voltage drops at the onset of the stimuli. According to our results, the steeper response was exhibited by ODR. However, we need a significantly larger data set to draw reliable conclusions about the nature of mechanosensors present on the flagellum.

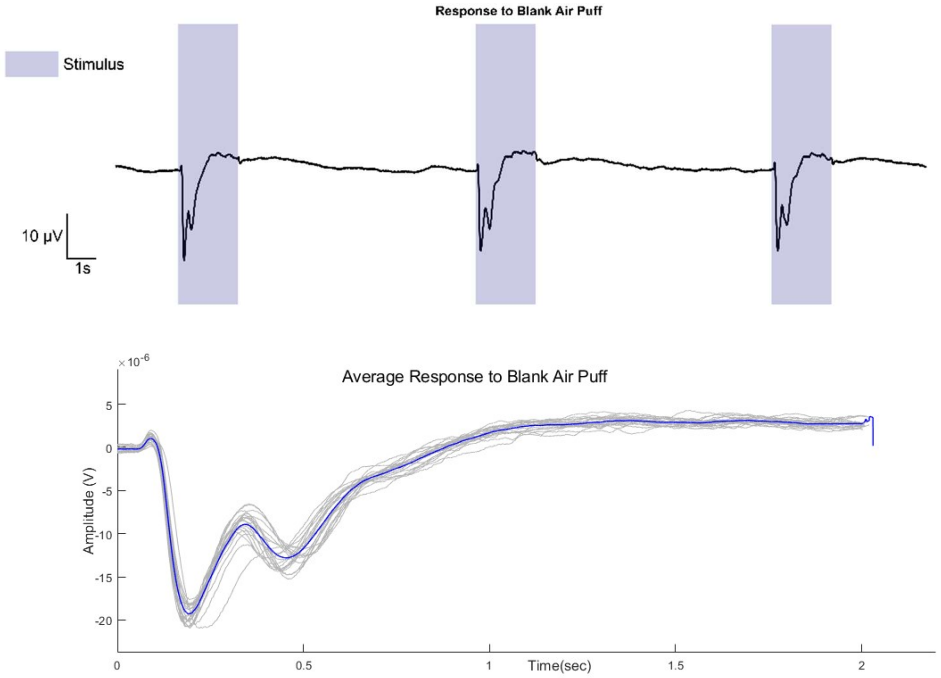

Fig 14: EAG (Electroantennogram) responses to blank air puff (Nitrogen). *(a) There is a drop in potential when stimulus (duration=2s) is delivered. (b) EAG responses across 10 trials denoted by grey traces. Blue trace denotes the mean EAG response blank air puff.*

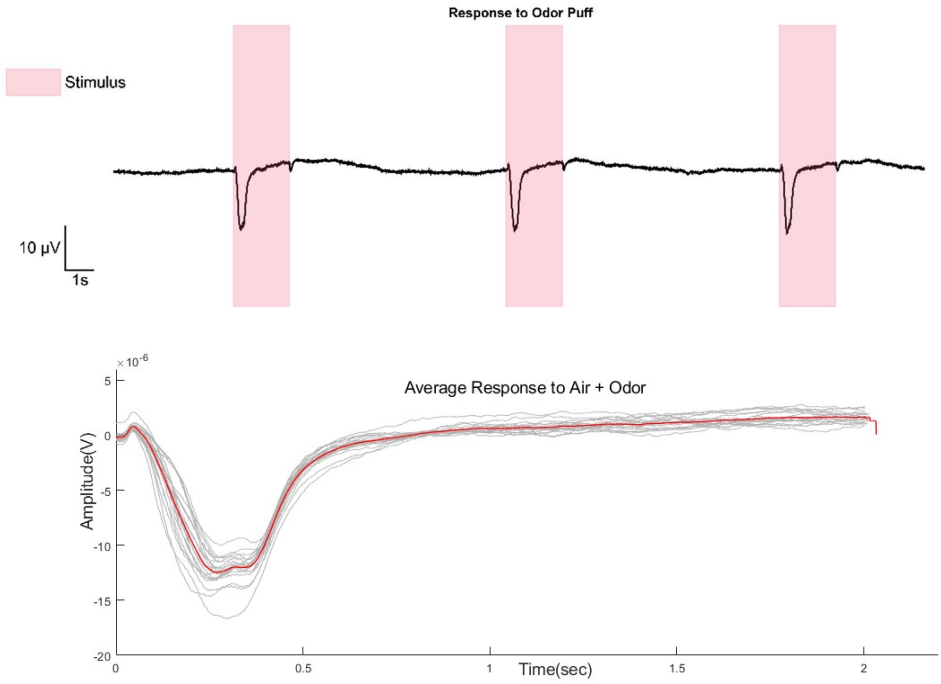

Fig 15: EAG (Electroantennogram) response to odour puff (Nitrogen + Linalool). *(a) There is a drop in potential when stimulus (duration=2s) is delivered. (b) EAG responses across 10 trials denoted by grey traces. Red trace denotes the mean EAG response to odour puff.*

4. DISCUSSION AND FUTURE DIRECTIONS

4.1 Scanning Electron Microscopy (SEM)

The base and shaft characteristics of the putative mechanosensors (morphology, width, length) are shared by sensilla chaetica described in the antennal flagella of hawkmoths (Lee and Strausfeld, 1990) and cockroaches (Nishino et al., 2005). In males, the putative mechanosensors are located near the boundary of leading and trailing edge of the antennae. This location is consistent across all annuli. These observations are consistent with a previous study in Tobacco hawkmoth (*Manduca sexta*), which noted similar location for sensilla chaetica through acetylcholinesterase (AchE) staining (Stengl et al., 1990). The scanning electron micrographs in our study provide us with a clear way to visualise the morphology and location of these sensors.

In addition, the base of the putative mechanosensor has a distinct raised nearly circular socket similar to that of individual Böhm's bristles which are also mechanosensory (Sant and Sane, 2018). In the noctuid moth *Heliothis virescens,* flagellar sensilla chaetica respond to certain compounds only when it is contact with them, hence they are classified as contact chemosensory or gustatory receptors (Jørgensen et al., 2007). This similarity to the previously described sensilla chaetica type-I in literature indicates that the observed sensory structures may be purely mechanosensory or gustatory.

4.2 Neuroanatomy

The antennal lobe of *D.nerii* contains multiple glomeruli. As described in an ultrastructural study in *M.sexta*, each glomerulus is a neuropil subunit where antennal sensory axons synapse with dendrites of antennal interneurons (Tolbert and Hildebrand, 1981). Among these glomeruli, there is a male-specific neuropil region called macroglomerular complex (MGC), where the pheromone-sensitive sensory neurons arborize (Christensen and Hildebrand, 1987). Fluorescent labelling of the antennal sensory neurons shows numerous arbors in the antennal lobe in both female and male moths. These are most likely the projection patterns of the abundant olfactory sensors on the flagellum (Homberg et al., 1989). However, a study conducted in the noctuid moth *Spodoptera littoralis* showed that a receptor neuron that responds to only mechanical stimuli arborizes in the Antennal lobe (AL) (Han et al., 2005), which suggests the presence of multisensory neurons in the AL.

Flagellar nerve also projects in the ipsilateral AMMC. These neurons bypass AL laterally before reaching AMMC. Previous studies have revealed similar projections patterns of flagellar sensory neurons in the AMMC (also called the 'dorsal lobe') in silk moths (*Bombyx mori*) (Koontz and Schneider, 1987). This is interesting because AMMC also receives projections from neurons innervating other antennal mechanosensory structures such as Böhm's bristles and Johnston's organs project (Sant and Sane, 2018; Krishnan et al., 2012), implying that these projections are mechanosensory receptors from flagellum. A definite test that they indeed are mechanosensory in nature would require a physiological readout.

After passing through the AMMC, there are thin fibres projecting onto the ipsilateral and contralateral SEZ region. Single sensillum dye labelling of s.chaetica on the antennal flagellum in *Heliothis virescens* show that it arborizes in the AMMC and ipsilateral SEZ of the brain (Jørgensen et al., 2006). The location and sensor morphologies of flagellar sensilla chaetica in *H.virescens* are comparable to that of the putative mechanosensors on the flagellum of *D.nerii* suggesting similarities in the underlying arborization patterns. Sensilla-specific dye filling is required for further investigation into the comparative aspects of the circuitry.

In the SEZ, we observe thin neural fibres projecting onto the contralateral side. Similar results are seen in the studies on honeybees (*Apis mellifera*) where antennal sensory neurons arborize in the contralateral SEZ (Arnold et al., 1985; Brockmann and Robinson, 2007). In some insects, arborisations in SEZ from the sensors on the antennal flagellum and labial palps along with motor neurons indicate towards its involvement in the proboscis extension reflex behaviour. (*Heliothis virescens*: Jørgensen et al., 2006; *Apis mellifera*: Rehder, 1989). However, we cannot correlate the arbors in the brain we see from the whole antennae fills in *D.nerii* to any particular behaviour on the basis of the present material.

The sensory neurons innervating the flagellum enter the mesothoracic ganglion (T2) after passing through the foramen separating the prothoracic ganglion (T1) and the mesothoracic ganglion (T2) and metathoracic ganglion (T3). Thus, the information sensed by the flagellum is transmitted posteriorly to the T2/T3, where it may interact – either directly or indirectly - with a motor neuron or an interneuron. Unfortunately, we were unable to further investigate their downstream targets since the Texas Red dextran dye does not cross synapses.

A limitation of this experiment was that the period of time required for the dye to diffuse passively was long enough to induce extensive neuronal death and blebbing in our samples. One way to minimize such large scale neuronal death due to extended periods of time after antennal nerve injury is to induce active dye perfusion through methods like current injection.

4.3 Electroantennogram (EAG)

Our preliminary analysis cannot claim there is any significant difference between responses to odour and blank air despite the differences we observe in the parameters associated with ODR and BLR. The dataset is based on 1 antenna and we need to increase the sample size to draw conclusive inferences.

A potential drawback of this experiment could have been effect of residual odour in the valves. This could have led to the 'blank air puff' carrying some odour molecules and stimulating the chemosensors. Therefore, the BLR we observed need not be purely mechanosensory. In the future experiments, we can ensure that this effect is minimized by allowing enough time gap between odour puffs and blank air puffs in addition to actively removing odour from the area using exhaust fan.

During the course of the experiment, we were able to create a circuit for the driver system to deliver controlled air puff stimuli. With the integration of this driver system, we now have an experimental setup to study EAG responses to air puff stimulus. However, this setup needs rigorous calibration before the next set of experiments.

The EAG responses to air puff stimuli can be extended to female moths in the future to inspect any sex-bias in the responses to mechanical stimuli. In our experiment, we kept the air flow rate constant. In the upcoming projects, we can study changes in EAG responses to different air flow rates (air speeds). In this way, we can study the sensitivity of flagellar mechanosensors to different air speeds. Another direction we could pursue are frequency dependent responses. As demonstrated in *M. sexta*, odour detection is maximized when odour pulses arrive at the wing beat frequency (Daly et al., 2013). It will be interesting if such correlation existed between frequencies of blank air puffs vs. flagellar mechanosensory responses.

5. REFERENCES

1. Altman, J. S., & Tyrer, N. M. (1980). Filling selected neurons with cobalt through cut axons. In *Neuroanatomical techniques* (pp. 373-402). Springer, New York, NY.
2. Arbas, E. A. (1986). Control of hindlimb posture by wind-sensitive hairs and antennae during locust flight. *Journal of Comparative Physiology A*, *159*(6), 849-857.
3. Arnold, G., Masson, C., & Budharugsa, S. (1985). Comparative study of the antennal lobes and their afferent pathway in the worker bee and the drone (Apis mellifera). *Cell and tissue research*, *242*(3), 593-605.
4. Barry, M. W., & Nielsen, D. G. (1984). Behavior of adult peachtree borer (Lepidoptera: Sesiidae). *Annals of the Entomological Society of America*, *77*(3), 246-250.
5. Böröczky, K., Wada-Katsumata, A., Batchelor, D., Zhukovskaya, M., & Schal, C. (2013). Insects groom their antennae to enhance olfactory acuity. *Proceedings of the national Academy of Sciences*, *110*(9), 3615-3620.
6. Brockmann, A., & Robinson, G. E. (2007). Central projections of sensory systems involved in honey bee dance language communication. *Brain, behavior and evolution*, *70*(2), 125-136.
7. Burdohan, J. A., & Comer, C. M. (1996). Cellular organization of an antennal mechanosensory pathway in the cockroach, Periplaneta americana. *Journal of Neuroscience*, *16*(18), 5830-5843.
8. Callahan, P. S., & Carlysle, T. C. (1971). A function of the epiphysis on the foreleg of the corn earworm moth, *Heliothis zea*. *Annals of the Entomological Society of America*, *64*(1), 309-311.
9. Christensen, T. A., & Hildebrand, J. G. (1987). Male-specific, sex pheromone-selective projection neurons in the antennal lobes of the moth Manduca sexta. *Journal of comparative Physiology A*, *160*(5), 553-569.
10. Daly, K. C., Kalwar, F., Hatfield, M., Staudacher, E., & Bradley, S. P. (2013). Odor detection in Manduca sexta is optimized when odor stimuli are pulsed at a frequency matching the wing beat during flight. *PLoS One*, *8*(11).

11. D'Ettorre, P., Heinze, J., Schulz, C., Francke, W., & Ayasse, M. (2004). Does she smell like a queen? Chemoreception of a cuticular hydrocarbon signal in the ant Pachycondyla inversa. *Journal of Experimental Biology*, *207*(7), 1085-1091.
12. Dieudonné, A., Daniel, T. L., & Sane, S. P. (2014). Encoding properties of the mechanosensory neurons in the Johnston's organ of the hawk moth, Manduca sexta. *Journal of Experimental Biology*, *217*(17), 3045-3056.
13. Eaton, J. L. (1974). Nervous system of the head and thorax of the adult tobacco hornworm, Manduca sexta (Lepidoptera: Sphingidae). *International Journal of Insect Morphology and Embryology*, *3*(1), 47-66.
14. Han, Q., Hansson, B. S., & Anton, S. (2005). Interactions of mechanical stimuli and sex pheromone information in antennal lobe neurons of a male moth, Spodoptera littoralis. *Journal of Comparative Physiology A*, *191*(6), 521-528.
15. Hlavac, T. F. (1975). Grooming systems of insects: structure, mechanics. *Annals of the Entomological Society of America*, *68*(5), 823-826.
16. Homberg, U., Christensen, T. A., & Hildebrand, J. G. (1989). Structure and function of the deutocerebrum in insects. *Annual review of entomology*, *34*(1), 477-501.
17. Horseman, B. G., Gebhardt, M. J., & Honegger, H. W. (1997). Involvement of the suboesophageal and thoracic ganglia in the control of antennal movements in crickets. *Journal of Comparative Physiology A*, *181*(3), 195-204.
18. Ito, K., Shinomiya, K., Ito, M., Armstrong, J. D., Boyan, G., Hartenstein, V., ... & Keshishian, H. (2014). A systematic nomenclature for the insect brain. *Neuron*, *81*(4), 755-765.
19. Jørgensen, K., Almaas, T. J., Marion-Poll, F., & Mustaparta, H. (2007). Electrophysiological characterization of responses from gustatory receptor neurons of sensilla chaetica in the moth Heliothis virescens. *Chemical senses*, *32*(9), 863-879.
20. Jørgensen, K., Kvello, P., Almaas, T. J., & Mustaparta, H. (2006). Two closely located areas in the suboesophageal ganglion and the tritocerebrum receive projections of gustatory receptor neurons located on the antennae and the proboscis in the moth Heliothis virescens. *Journal of Comparative Neurology*, *496*(1), 121-134.

21. Kaissling, K. E. (1995). 4.19. Single unit and Electrontennogram recordings in insect olfactory organs. *Experimental cell biology of taste and olfaction: current techniques and protocols*, 361.
22. Kaissling, K. E., & Thorson, J. O. H. N. (1980). Insect olfactory sensilla: structural, chemical and electrical aspects of the functional organisation. In *Receptors for neurotransmitters, hormones and pheromones in insects* (pp. 261-282). Elsevier/North-Holland Biomedical Press.
23. Kamikouchi, A., Inagaki, H. K., Effertz, T., Hendrich, O., Fiala, A., Göpfert, M. C., & Ito, K. (2009). The neural basis of Drosophila gravity-sensing and hearing. *Nature*, *458*(7235), 165-171.
24. Khurana, T. R., & Sane, S. P. (2016). Airflow and optic flow mediate antennal positioning in flying honeybees. *Elife*, *5*, e14449.
25. Koontz, M. A., & Schneider, D. (1987). Sexual dimorphism in neuronal projections from the antennae of silk moths (Bombyx mori, Antheraea polyphemus) and the gypsy moth (Lymantria dispar). *Cell and tissue research*, *249*(1), 39-50.
26. Krishnan, A., Prabhakar, S., Sudarsan, S., & Sane, S. P. (2012). The neural mechanisms of antennal positioning in flying moths. *Journal of Experimental Biology*, *215*(17), 3096-3105.
27. Lee, J. K., & Strausfeld, N. J. (1990). Structure, distribution and number of surface sensilla and their receptor cells on the olfactory appendage of the male moth *Manduca sexta*. *Journal of neurocytology*, *19*(4), 519-538.
28. Lusebrink I, Dettner K, Seifert K (2008) Stenusine, an antimicrobial agent in the rove beetle genus Stenus (Coleoptera, Staphylinidae). Naturwissenschaften 95(8):751–755.
29. Nishino, H., Nishikawa, M., Yokohari, F., & Mizunami, M. (2005). Dual, multilayered somatosensory maps formed by antennal tactile and contact chemosensory afferents in an insect brain. *Journal of Comparative Neurology*, *493*(2), 291-308.
30. Okada, J., & Toh, Y. (2000). The role of antennal hair plates in object-guided tactile orientation of the cockroach (Periplaneta americana). *Journal of Comparative Physiology A*, *186*(9), 849-857.

31. Park, K. C., Ochieng, S. A., Zhu, J., & Baker, T. C. (2002). Odor discrimination using insect electroantennogram responses from an insect antennal array. *Chemical senses*, *27*(4), 343-352.
32. Rehder, V. (1989). Sensory pathways and motoneurons of the proboscis reflex in the suboesophageal ganglion of the honey bee. *Journal of Comparative Neurology*, *279*(3), 499-513.
33. Rohrseitz, K., & Tautz, J. (1999). Honey bee dance communication: waggle run direction coded in antennal contacts?. *Journal of Comparative Physiology A*, *184*(4), 463-470.
34. Sane, S. P., Dieudonné, A., Willis, M. A., & Daniel, T. L. (2007). Antennal mechanosensors mediate flight control in moths. *Science*, *315*(5813), 863-866.
35. Sanes, J. R., & Hildebrand, J. G. (1976). Structure and development of antennae in a moth, *Manduca sexta*. *Developmental biology*, *51*(2), 282-299.
36. Sant, H. H., & Sane, S. P. (2018). The mechanosensory-motor apparatus of antennae in the Oleander hawk moth (Daphnis nerii, Lepidoptera). *Journal of Comparative Neurology*, *526*(14), 2215-2230.
37. Sant, H. H., & Sane, S. P. (2019). 19 A Comparative Study of Antennal Mechanosensors in Insects. *Indian Insects: Diversity and Science*, 389.
38. Schneider, D. (1957). Electrophysiological investigation on the antennal receptors of the silk moth during chemical and mechanical stimulation. *Experientia*, *13*(2), 89-91.
39. Schneider, D. (1964). Insect antennae. *Annual review of entomology*, *9*(1), 103-122.
40. Schütz, C., & Dürr, V. (2011). Active tactile exploration for adaptive locomotion in the stick insect. *Philosophical Transactions of the Royal Society B: Biological Sciences*, *366*(1581), 2996-3005.
41. Schweitzer, E. S., Sanes, J. R., & Hildebrand, J. G. (1976). Ontogeny of electroantennogram responses in the moth, Manduca sexta. *Journal of insect physiology*, *22*(7), 955-960.
42. Seeds, A. M., Ravbar, P., Chung, P., Hampel, S., Midgley Jr, F. M., Mensh, B. D., & Simpson, J. H. (2014). A suppression hierarchy among competing motor programs drives sequential grooming in Drosophila. *Elife*, *3*, e02951.

43. Staudacher, E. M., Gebhardt, M., & Dürr, V. (2005). Antennal movements and mechanoreception: neurobiology of active tactile sensors. *Advances in insect physiology*, *32*, 49-205.
44. Stengl, M., Homberg, U., & Hildebrand, J. G. (1990). Acetylcholinesterase activity in antennal receptor neurons of the sphinx moth *Manduca sexta*. *Cell and tissue research*, *262*(2), 245-252.
45. Tolbert, L. P., & Hildebrand, J. G. (1981). Organization and synaptic ultrastructure of glomeruli in the antennal lobes of the moth Manduca sexta: a study using thin sections and freeze-fracture. *Proceedings of the Royal Society of London. Series B. Biological Sciences*, *213*(1192), 279-301.
46. Yorozu, S., Wong, A., Fischer, B. J., Dankert, H., Kernan, M. J., Kamikouchi, A., ... & Anderson, D. J. (2009). Distinct sensory representations of wind and near-field sound in the Drosophila brain. *Nature*, *458*(7235), 201-205.
47. Zhukovskaya, M., Yanagawa, A., & Forschler, B. (2013). Grooming behavior as a mechanism of insect disease defense. *Insects*, *4*(4), 609-630.

...